Physics beyond the standard model with kaons at NA62

Cite as: AIP Conference Proceedings **2249**, 030003 (2020); https://doi.org/10.1063/5.0009508
Published Online: 27 July 2020

Paolo Massarotti, and on behalf of NA62 Collaboration

Physics beyond the Standard Model with kaons at NA62

Paolo Massarotti[1, 2, a)] on behalf of NA62 Collaboration

[1)]*Dipartimento di Fisica "Ettore Pancini" dell'Universitá degli Studi di Napoli Federico II, Italia.*
[2)]*Istituto Nazionale di Fisica Nucleare, Sezione di Napoli, Italia*

.

[a)]*Corresponding author:massarotti@na.infn.it*

Abstract. The NA62 experiment at CERN Super Proton Synchrotron was designed to measure BR($K^+ \to \pi^+ \nu\bar{\nu}$) with an in-fight technique, never used before for this measurement. This decay is characterised by a very precise prediction in the Standard Model. Its branching ratio, which is expected to be less than 10^{-10}, is one of the best candidates to indicate indirect effects of new physics beyond SM at the highest mass scales. NA62 result on $K^+ \to \pi^+ \nu\bar{\nu}$ from the full 2016 data set is described.
Also a search for an invisible dark photon A' has been performed, exploiting the efficient photon-veto capability and high resolution tracking of the NA62. The signal stems from the chain $K^+ \to \pi^+\pi^0$ followed by $\pi^0 \to A'\gamma$. No significant statistical excess has been identified. Upper limits on the dark photon coupling to the ordinary photon as a function of the dark photon mass have been set, improving on the previous limits over the mass range 60 - 110 MeV/c^2.

THE NA62 EXPERIMENT AT CERN

The fixed target NA62 experiment aims at measuring the branching ratio of the decay $K^+ \to \pi^+ \nu\bar{\nu}$ ($K_{\pi\nu\bar{\nu}}$) with a 10% precision. A sample of about 10^{13} kaon decays should be collected in few years and a maximum of 10% of background contamination is required, necessitating a background rejection factor of the order of 10^{12}. The experiment is located in the North Area of CERN; here, a primary beam of protons with a momentum of 400 GeV/c hits a beryllium target to create a non-separated beam of hadrons of 75 GeV/c momentum. This secondary beam, made of pions (70%), protons (23%) and kaons (6%) reaches the 260 m long apparatus of NA62, shown in figure 1. The experimental technique

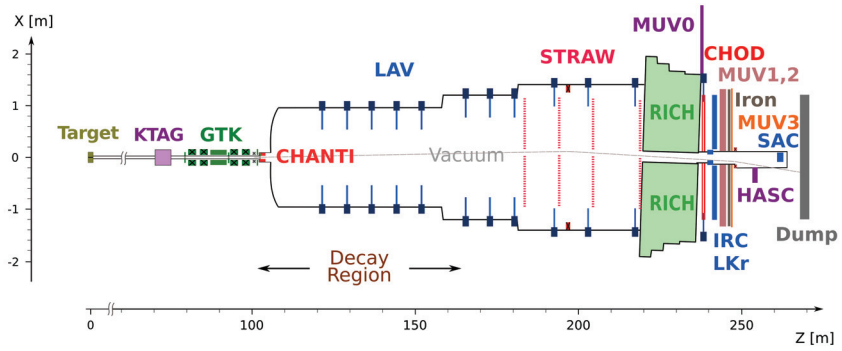

FIGURE 1. A schematic illustration of NA62 apparatus in x-z plane.

used by NA62 is the in-flight detection of kaon decays in a 80 m long fiducial volume. Kaons are identified by a Cherenkov differential counter (KTAG) which also provides timestamps for them. Kaon momentum is measured by the GigaTracKer (GTK), a three-station silicon spectrometer. To reject background coming from inelastic interactions between the kaons and the GTK, a veto detector (CHANTI) is located downstream the last station of the tracker. The momenta of the downstream particles are measured by a straw tubes spectrometer, (STRAW). A Ring Imaging CHerenkov detector (RICH) provides π^+ identification and reject e^+ and μ^+. Fast timing informations come from the RICH and a scintillation hodoscope (CHOD), placed downstream to it. A background rejection factor at the order of 10^{12} is required to separate the signal from the other kaon decays, whose BRs are several order of magnitudes higher than the signal, like $K^+ \to \mu^+\nu$ ($K_{\mu 2}$, $BR = 63\%$) and $K^+ \to \pi^+\pi^0$ ($K_{\pi 2}$, $BR = 21\%$). Two hadronic calorimeters (MUV1 and MUV2) and a fast scintillator array (MUV3) provide further separation between π^+ and μ^+. A set of photons vetoes (LAVs, LKr, IRC, SAC) hermetically cover angles up to 50 mrad to reject extra electromagnetic activity. A more detailed description of NA62 apparatus can be found in [1] .

Proceedings of the 15th International Conference on Meson-Nucleon Physics and the Structure of the Nucleon
AIP Conf. Proc. 2249, 030003-1–030003-7; https://doi.org/10.1063/5.0009508
Published by AIP Publishing. 978-0-7354-2008-3/$30.00

THE $K^+ \to \pi^+ \nu\bar{\nu}$ DECAY

The rare decay $K^+ \to \pi^+ \nu\bar{\nu}$ ($K_{\pi\nu\bar{\nu}}$) is a golden channel for high-precision tests of the Standard Model (SM). It is a Flavour Changing Neutral Current (FCNC) process, forbidden at the tree-level in the SM. The decay can be described by a short-distance effective hamiltonian in which the main contribution comes from top quark loops with a sub-leading contribution from charm. The hadronic matrix element can be related via isospin symmetry to the one of K^+_{e3} decay, measured with good accuracy. For this reason, the prediction is essentially not affected by hadronic uncertainties. This makes the $K_{\pi\nu\bar{\nu}}$ very clean theoretically and sensitive to physics beyond the SM. The SM prediction for the Branching Ratio (BR) of $K_{\pi\nu\bar{\nu}}$ is [2]:

$$BR(K_{\pi\nu\bar{\nu}}) = (8.4 \pm 1.0) \times 10^{-11}. \quad (1)$$

The knowledge of the external inputs dominates the uncertainties on the predictions. Experiments E787 and E949 at Brookhaven National Laboratory performed a measurement of this BR using stopped kaons; the result was [3]:

$$BR(K_{\pi\nu\bar{\nu}}) = (1.73^{+1.15}_{-1.05}) \times 10^{-10}. \quad (2)$$

The branching ratio is $\sim 1\sigma$ away from the SM prediction, but the measurement was based on only few events and the experimental uncertainties are large.

K$\to \pi\nu\bar{\nu}$ analisys

The analysis of the complete 2016 data set, corresponding to a total number of kaon decays in the fiducial decay region $N_K = 1.21(2)\times10^{11}$, is presented [4]. The $K_{\pi\nu\bar{\nu}}$ decay signature is one track with two missing neutrinos. The main kinematic variable is $m^2_{miss} \equiv (p_K - p_{\pi^+})^2$, where p_K and p_{π^+} are the 4-momenta of the K^+ and π^+ respectively. The theoretical shape of the principal K^+ background decay modes are compared to the $K_{\pi\nu\bar{\nu}}$ in figure 2-left. The

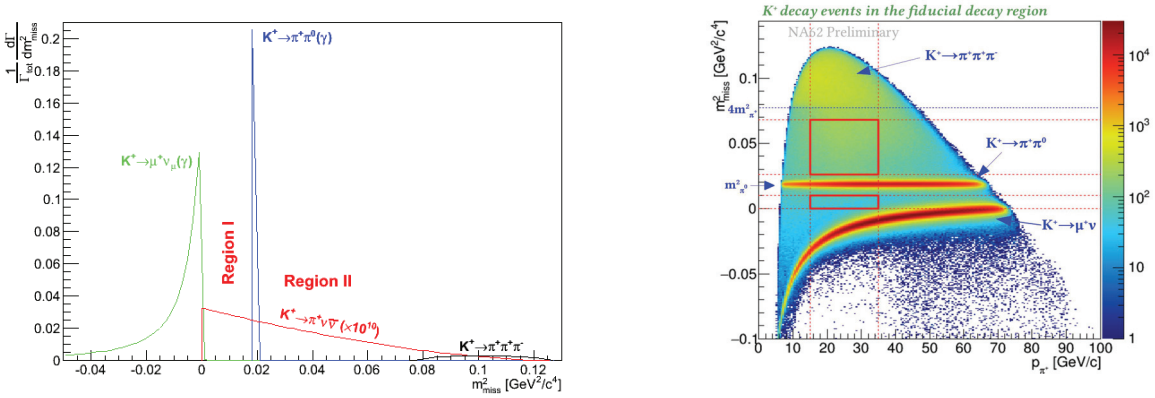

FIGURE 2. Left: m^2_{miss} shapes for signal and $K_{\mu2}$ and $K_{\pi2}$ backgrounds: the backgrounds are normalised according to their branching ratio; the signal is multiplied by a factor 10^{10}. Right: Distribution of m^2_{miss} as a function of track momentum for events selected on minimum bias data; The bands corresponding to $K_{\mu2}$ and $K_{\pi2}$ decays are clearly visible; the signal regions (red box) are drawn for reference.

analysis is performed in two separate regions: Region 1 (R1), between the $K_{\mu2}$ and $K_{\pi2}$ contribution, and Region 2 (R2) between $K_{\pi2}$ and $K \to \pi^+\pi^+\pi^-(K_{3\pi})$ contribution. The main backgrounds in these regions are $K_{\mu2}$ and $K_{\pi2}$ decays characterised by non-gaussian resolution or radiative tails , $K_{3\pi}$ decays characterised by non-gaussian momentum resolution, $K \to \pi^+\pi^- e^+ \nu_e$ (K_{e4}) decays, K^+ decays upstream of the GTK3 station and inelastic beam-detector interactions. Each of the background processes requires different rejection procedure according to its kinematics and to the type of charged particle in the final state. Events with single track topology are selected using the downstream detectors STRAW, CHOD and RICH. The track is required to match with the CHOD and to have a reconstructed ring in the RICH, which is characterised by a time resolution of the order of 100 ps. The downstream track is then associated to an in-time kaon in the KTAG detector and associated to a the corresponding K^+ track in the GTK detector.

A kaon decay vertex is created at the intersection point of the GTK and STRAW tracks. The kaon decays within a 50 m fiducial region, beginning 10 m downstream to the last GTK station (GTK3), are selected (figure 2-right). The calorimeters and the RICH identify the π^+ tracks providing 10^8 μ suppression with 64%π^+ efficiency. These performances are measured on kinematically selected $K_{\mu 2}$ and $K_{\pi 2}$ decays on control-trigger data. Events passing the π^+ identification criteria are mainly $K_{\pi 2}$ decays, which are further suppressed by looking for energy deposits in the electromagnetic calorimeters in-time with the π^+. The π^0 suppression is of the order of 3×10^8, as measured directly on data. Signal region definitions are driven by the m^2_{miss} resolution $\sigma_{m^2_{miss}} = 10^3$ GeV^2/c^4. The total $K_{\pi\nu\bar{\nu}}$ acceptance, taking into account signal region definition and selection cuts, is 4%, R1(1%) and R2(3%).
The probability of the $K_{\mu 2}$ ($K_{\pi 2}$) decays to enter the signal regions 3×10^{-4} (1×10^{-3}). This kinematic suppression factor is measured using $K_{\mu 2}$ ($K_{\pi 2}$) decays selected with $K_{\pi\nu\bar{\nu}}$ like selection on a control-trigger data sample.
The Single Event Sensitivity (SES) for a SM $K_{\pi\nu\bar{\nu}}$ decay is SES = $(3.15\pm0.01_{stat}\pm0.24_{syst})\times10^{-10}$, dominated by systematic uncertainty. Summary of the systematic uncertainties on the SES is presented in TABLE I.

Source	δ SES (10^{-10})
Random veto	$\pm$ 0.17
Denition of $\pi^+\pi^0$ region	$\pm$ 0.10
$A_{\pi\nu\bar{\nu}}$	$\pm$ 0.09
N_K	$\pm$ 0.05
Trigger efficiency	$\pm$ 0.04
Extra activity	$\pm$ 0.02
Pileup simulation	$\pm$ 0.02
Momentum spectrum	$\pm$ 0.01
Total	$\pm$ 0.024

TABLE I. Sources of systematic uncertainties to SES: The uncertainty is dominated by random veto losses induced by the π^0 rejection, stability of the SES estimation varying the $\pi^+\pi^0$ normalisation region, simulation of the π^+ losses due to interactions in the detector material upstream of the hodoscopes.

The behaviour of the $K_{\pi 2(\gamma)}$ and $K_{\mu 2(\gamma)}$ background decays is shown in figure 3 as a function of the P_{π^+} momentum and compared to the signal expectation. The $K_{\pi 2(\gamma)}$ ($K_{\mu 2(\gamma)}$) background is dominating at low (high) P_{π^+}. A MC simulation of 400 million generated K_{e4} decays is used to estimate the expected background. The upstream background is estimated using a data driven method.

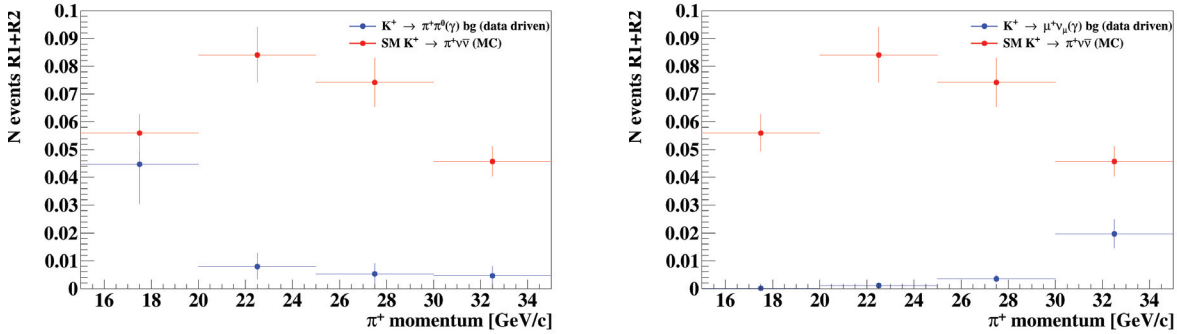

FIGURE 3. Left: Expected number of $K_{\pi 2(\gamma)}$ background events in R1 and R2 in bins of P_{π^+} compared to the expected number of SM $K_{\pi\nu\bar{\nu}}$ events. Right: Expected number of $K_{\mu 2(\gamma)}$ background. Uncertainties on the background estimations are statistical only, while on expected signal are mostly systematic.

K$\to \pi\nu\bar{\nu}$ Results with 2016 data set

One event has been found in R2 after un-blinding the signal regions. The $K_{\pi\nu\bar{\nu}}$ candidate event, figure 4-left, is consistent with a π^+ track in the RICH detector, figure 4-right.

Process	Expected events in R1+ R2
$K_{\pi\nu\bar{\nu}}$ (SM)	$0.267 \pm 0.001_{stat} \pm 0.020_{syst}\ pm\ 0.032_{ext}$
$K_{\pi 2(\gamma)}$ IB	$0.604 \pm 0.007_{stat} \pm 0.006_{syst}$
$K_{\mu 2(\gamma)}$ IB	$0.020 \pm 0.003_{stat} \pm 0.003_{syst}$
K_{e4}	$0.018^{+0.024}_{-0.017}\|_{stat} \pm 0.009_{syst}$
$K_{3\pi}$	$0.002 \pm 0.001_{stat} \pm 0.002_{syst}$
Upstream Background	$0.050^{+0.090}_{-0.030}\|_{stat}$
Total Background	$0.15 \pm 0.09_{stat} \pm 0.01_{syst}$

TABLE II. Expected number of signal and background events in R1 and R2 on the complete 2016 data set.

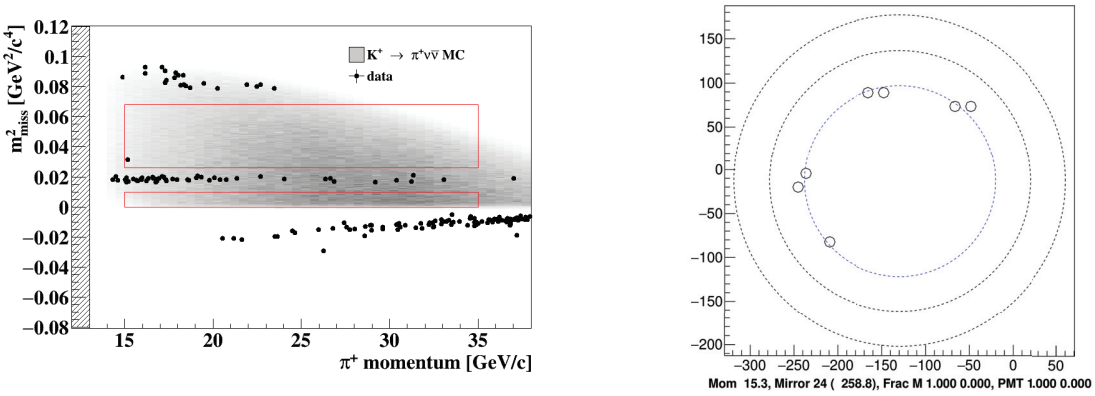

FIGURE 4. Left: m^2_{miss} as a function of P_{π^+} after applying the $K_{\pi\nu\bar{\nu}}$ selection, but the cuts on m^2_{miss} and P_{π^+}. The grey area is given by $K_{\pi\nu\bar{\nu}}$ MC events. The red lines correspond to the signal regions. The event observed in R2 is shown. Right: Position of the hits in the RICH forming the ring associated to the π^+ track for the observed event in R2. The circles illustrate the positron (outermost ring), muon and pion (the innermost ring) hypothesis, showing a perfect agreement with the pion hypothesis.

Upper limit on the branching ratio of the $K_{\pi\nu\bar{\nu}}$ decay are obtained using the CLs method:

$$BR(K_{\pi\nu\bar{\nu}}) < 11 \times 10^{-10} @ 90\% CL \tag{3}$$

$$BR(K_{\pi\nu\bar{\nu}}) < 14 \times 10^{-10} @ 95\% CL \tag{4}$$

A measurement of the branching ratio at 68% CL is also computed

$$BR(K_{\pi\nu\bar{\nu}}) = 2.8^{+4.4}_{-2.3} \times 10^{-10} @ 68\% CL \tag{5}$$

The branching ratio estimation has been shown only for comparison with the Standard Model prediction, Equation 1, and with the result obtained by the BNL E949 collaboration, Equation 2. This result is in agreement with both the SM prediction and previous measurements. Improvements at both hardware and analysis level are foreseen to reduce the background and improve signal efficiency. NA62 should observe about 20 SM $K_{\pi\nu\bar{\nu}}$ events with the complete data set, considering the statistics collected in 2017 and expected in 2018.

A' SEARCH

The LHC explored a large new territor and no unambiguous signal of new physics (NP) has been found. However some yet unknown particles or interactions are required to explain a number of observed phenomena in particle physics like the neutrino masses and oscillations, the baryon asymmetry of the universe, the dark matter and energy. Complemetary approaches to LHC in the intensity frontier field allow us to explore NP effects using high-rate environment and looking for very rare processes.

To explain the abundance of dark matter in our universe, SM can be extended using a new $U(1)$ gauge-symmetry sector, with a vector mediator field A' named as "dark photon" with mass $M_{A'}$. In a simple realization of such

a scenario [5, 6], the A' field would feebly interact with the SM photon through a kinetic mixing lagrangian with a coupling parameter ε. The above lagrangian should describe interactions both with SM matter fields and with a hidden sector of possible dark-matter candidate fields. If these are lighter than the A', the dark photon would decay mostly invisibly, so that a missing-energy signature might reveal its presence. In this study [7], an A' search is performed, with A' escaping detection from the decay chain

$$K^+ \to \pi^+\pi^0 \text{ with } \pi^0 \to A'\gamma, \tag{6}$$

where

$$\mathrm{BR}\left(\pi^0 \to A'\gamma\right) = 2\varepsilon^2 \left(1 - \frac{M_{A'}^2}{M_{\pi^0}^2}\right)^3 \times \mathrm{BR}\left(\pi^0 \to \gamma\gamma\right) \tag{7}$$

The high-energy unseparated hadron beam from the CERN Super Proton Synchrotron (SPS) provides an abundant flux of K^+ mesons useful to this purpose. The A' search exploits the extreme photon-veto capability and high resolution tracking of the NA62 detector in a high-rate environment [1].

analysis strategy

If the A' decays into some invisible mode, the experimental signature for the events described in Eq. 6 is given by a charged kaon decaying into a charged pion and a photon hitting the liquid Krypton calorimeter (LKr), with missing energy and momentum. The kaon and pion momenta are measured with GTK and STRAW, respectively, and the corresponding 4-momenta are denoted P_K and P_π. The measurement of the position of impact and the energy released in the LKr calorimeter allow the determination of the photon 4-momentum P_γ, assuming emission from the kaon decay vertex. The squared missing mass

$$M_{\mathrm{miss}}^2 = \left(P_K - P_\pi - P_\gamma\right)^2 \tag{8}$$

is expected to peak at $M_{A'}^2$ for the decay chain in Eq. 6 and at zero for the most abundant background, $\pi^0 \to \gamma\gamma$ with one photon undetected.

A high-purity kinematic identification of the $K^+ \to \pi^+\pi^0$ decays is performed by identifying and reconstructing the K^+ and π^+ particles and requiring $(P_K - P_\pi)^2$ to be consistent with the squared π^0 mass. The number n_{π^0} of $K^+ \to \pi^+\pi^0$ decays defines the statistics of tagged π^0 mesons used for this analysis. In order to enforce the sole presence of a π^+ and one photon in the final state, further conditions are required and the most relevant are:

- No in-time signals from the photon veto system must be present, except for the ones related to the single photon and to the π^+ detected by the LKr.
- No in-time hits in the hodoscope (NA48-CHOD) before the LKr calorimeter must be found except for those geometrically associated with the π^+. This condition is useful to reject events in which one photon is lost because of conversion upstrem of the hodoscope.

A peak search in the positive tail of the M_{miss}^2 background distribution is performed by comparing the number of events in a sliding M_{miss}^2 window to the background expectation for different $M_{A'}$ hypothesis in the range 30-130 MeV$/c^2$.

For example, Fig. 5 shows the distributions of M_{miss}^2 from a Monte Carlo (MC) simulation of the NA62 apparatus when injecting A' signals with masses of 60, 90, and 120 MeV$/c^2$ and a coupling strength $\varepsilon^2 = 2.5 \times 10^{-4}$ (see Eq. 7). These are superimposed on the expected contribution from a data sample with fully reconstructed $\pi^0 \to \gamma\gamma$ in which one of the two photon hitting the LKr calorimeter, randomly chosen, is artificially excluded.

To evaluate the expected background, a data-driven approach is used. The same data selection used for the signal search is applied: events with in-time NA48-CHOD signals geometrically associated with the detected photon are rejected, while the presence of signals far from both the π^+ and photon impact points to the NA48-CHOD hodoscope is required. This allows the selection of a data control sample of $\pi^0 \to \gamma\gamma$ events with one photon detected by the LKr calorimeter and the other lost because of conversion upstream of the NA48-CHOD. Since there is no overlap with the signal sample, the control sample can be used to evaluate the expected M_{miss}^2 background distribution. The control sample is scaled to the signal sample in a side-band region adjacent to but not overlapping with the A' search region.

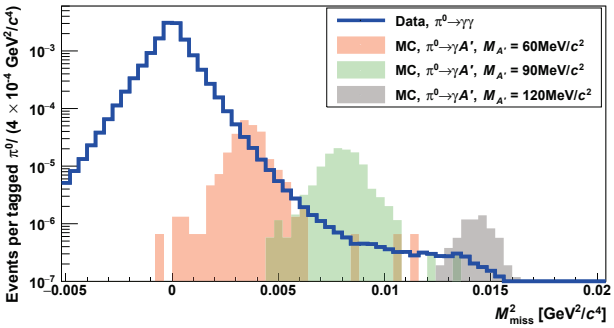

FIGURE 5. Distributions of the squared missing mass evaluated from K^+ decays with one photon and one π^+ reconstructed (Eq. 8). Data from $\pi^0 \to \gamma\gamma$ with one photon, randomly chosen, assumed to be undetected are shown by the blue line. The expected spectra from MC simulations of $\pi^0 \to A'\gamma$ with a coupling strength $\varepsilon^2 = 2.5\times10^{-4}$ and A' masses of 60 (red), 90 (green) and 120 MeV/c^2 (grey) are also shown. The data distribution is scaled to n_{π^0}. Each MC distribution is scaled to the equivalent number of tagged π^0 mesons corresponding to the generated statistics.

Results

The observed data and the expected background counts are evaluated by integrating the corresponding $M^2_{\rm miss}$ spectrum in the sliding window for each $M_{A'}$ hypothesis. The width of the sliding window is $\pm1\,\sigma_{M^2_{\rm miss}}$ around the expected $M^2_{\rm miss}$ peak value, where $\sigma_{M^2_{\rm miss}}$ is the resolution evaluated with MC simulations and checked with $K^+ \to \pi^+\pi^0$, $\pi^0 \to \gamma e^+e^-$ data sample.

Using the CL$_s$ algorithm, frequentist 90% confidence intervals are determined for the number of signal events. The upper limits are compatible within two standard deviations with the fluctuation expected in the background-only hypothesis. The 90% CL upper limits obtained on the coupling parameter ε^2 as a function of $M_{A'}$ are shown in figure , left. The limit from the number of observed events (solid curve) is compared to the bands with 68% and 95% coverage in the absence of signal and no statistically significant excess is detected [7]
. This NA62 result improves on the previous limits over the mass range 60–110 MeV/c^2(figure , right). It has to be

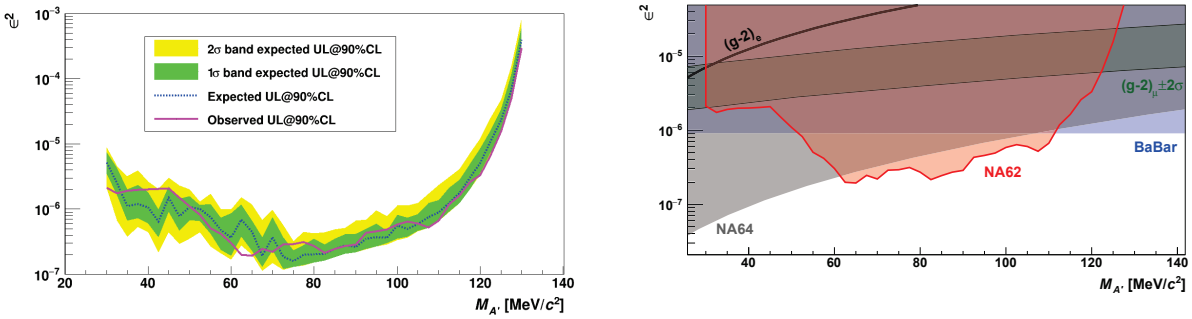

FIGURE 6. LEFT: upper limits at 90% CL on the dark photon coupling strength (ε^2) as a function of the mass ($M_{A'}$). The limit obtained from data (solid line) should be compared to that expected in the absence of signal: the median of the upper-limit distribution in the background-only hypothesis is shown by the dashed line and the corresponding fluctuation bands with 68% and 95% coverage are shown by the shaded areas. RIGHT: upper limit at 90% CL from NA62 (red region) in the ε^2 vs $M_{A'}$ plane with A' decaying into invisible final states. The limits from the BaBar [8] (blue) and NA64 [9] (light grey) experiments are shown. The green band shows the region of the parameter space corresponding to an explanation of the discrepancy between the measured and expected values of the anomalous muon magnetic moment $(g-2)_\mu$ in terms of a contribution from the A' in the quantum loops [10, 11]. The region above the black line is excluded by the agreement of the anomalous magnetic moment of the electron $(g-2)_e$ with its expected value [12, 13, 14].

underlined that the experimental technique used by NA62 is totally different than the one of the other recent results.

ACKNOWLEDGMENTS

The author thanks the NA62 Collaboration: R. Aliberti, F. Ambrosino, R. Ammendola, B. Angelucci, A. Antonelli, G. Anzivino, R. Arcidiacono, M. Barbanera, A. Biagioni, L. Bician, C. Biino, A. Bizzeti,T. Blazek, B. Bloch-Devaux, V. Bonaiuto, M. Boretto, M. Bragadireanu, D. Britton, F. Brizioli, M.B. Brunetti, D. Bryman, F. Bucci, T. Capussela, A. Ceccucci, P. Cenci, V. Cerny, C. Cerri,B. Checcucci, A. Conovalo, P. Cooper, E. Cortina Gil, M. Corvino, F. Costantini, A. Cotta Ramusino, D. Coward, G. DAgostini, J. Dainton, P. Dalpiaz, H. Danielsson, N. De Simone, D. Di Filippo, P. Laycock, L. Di Lella, N. Doble, B. Dobrich, F. Duval, V. Duk, J. Engelfried, T. Enik,N. Estrada-Tristan, V. Falaleev, R. Fantechi, V. Fascianelli, L. Federici, S. Fedotov, A. Filippi, M.Fiorini, J. Fry, J. Fu, A. Fucci, L. Fulton, E. Gamberini, L. Gatignon, G. Georgiev, S. Ghinescu, A.Gianoli, M. Giorgi, S. Giudici, F. Gonnella, E. Goudzovski, C. Graham, R. Guida, E. Gushchin, F.Hahn, H. Heath, T. Husek, O. Hutanu, D. Hutchcroft, L. Iacobuzio, E. Iacopini, E. Imbergamo, B.Jenninger, K. Kampf, V. Kekelidze, S. Kholodenko, G. Khoriauli, A. Khotyantsev, A. Kleimenova, A. Korotkova, M. Koval, V. Kozhuharov, Z. Kucerova, Y. Kudenko, J. Kunze, V. Kurochka,V.Kurshetsov, G. Lanfranchi, G. Lamanna, G. Latino, P. Laycock, C. Lazzeroni, G. Lehmann Miotto, M. Lenti, E. Leonardi, P. Lichard, L. Litov, R. Lollini, D. Lomidze, A. Lonardo, P. Lubrano, M. Lupi, N. Lurkin, D. Madigozhin, I. Mannelli, G. Mannocchi, A. Mapelli, F. Marchetto,R.Marchevski, S. Martellotti, P. Massarotti, K. Massri, E. Maurice, M. Medvedeva, A. Mefodev, E. Menichetti, E. Migliore, E. Minucci, M. Mirra, M. Misheva, N. Molokanova, M. Moulson, S. Movchan, M. Napolitano, I. Neri, F. Newson, A. Norton, M. Noy, T. Numao, V. Obraztsov, A.Ostankov, S. Padolski, R. Page, V. Palladino, C. Parkinson, E. Pedreschi, M. Pepe, M. Perrin-Terrin, L. Peruzzo, P. Petrov, F. Petrucci, R. Piandani, M. Piccini, J. Pinzino, I. Polenkevich, L.Pontisso, Yu. Potrebenikov, D. Protopopescu, M. Raggi, A. Romano, P. Rubin, G. Ruggiero, V.Ryjov, A. Salamon, C. Santoni, G. Saracino, F. Sargeni, V. Semenov, A. Sergi, A. Shaikhiev, S.Shkarovskiy, D. Soldi, V. Sougonyaev, M. Sozzi, T. Spadaro, F. Spinella, A. Sturgess, J. Swallow, S. Trilov, P. Valente, B. Velghe, S. Venditti, P. Vicini, R.Volpe, M. Vormstein, H. Wahl, R. Wanke, B. Wrona, O. Yushchenko, M. Zamkovsky, A. Zinchenko.

REFERENCES

1. E. Cortina-Gil and et al. [The NA62 Collaboration], "The beam and detector of the na62 experiment at cern," JINST **05**, P05025 (2017).
2. A. J. Buras, D. Buttazzo, J. Girrbach-Noe, and R. Knegjens, "$K^+ \to \pi^+ \nu\bar{\nu}$ and $K_l \to \pi^0 \nu\bar{\nu}$ in the standard model: status and perspectives," JHEP **1511**, 033 (2015).
3. A. V. Artamonov and et al [BNL-E949 Collaboration], "Study of the decay $k^+ \to \pi^+ \nu\bar{\nu}$ in the momentum region $140 < p_\pi < 199$ mev/c," Phys. Rev. D **79**, 092004 (2009).
4. E. Cortina-Gil and et al. [The NA62 Collaboration], "First search for $k^+ \to \pi^+ \nu\bar{\nu}$ using the decay-in-flight technique," Phys. Lett. B **791**, 156 (2019).
5. L. Okun, Sov. Phys. JETP **56**, 502 (1982).
6. B. Holdom, Phys. Lett. B. **166**, 196 (1986).
7. E. Cortina-Gil and et al. [The NA62 Collaboration], "Search for production of an invisible dark photon in π^0 decays," JHEP **1905**, 182 (2019).
8. J. P. Lees and et at [The BaBar Collaboration], Phys. Rev. Lett. **119**, 131804 (2017).
9. D. Banerjee and et al., Phys. Rev. D **97**, 072002 (2018).
10. P. Fayet, Phys. Rev. D **75**, 115017 (2007).
11. M. Pospelov, Phys. Rev. D **80**, 095002 (2009).
12. D. Hanneke, S. Fogwell, and G. Gabrielse, Phys. Rev. Lett. **100**, 120801 (2009).
13. R. Bouchendira and et al., Phys. Rev. Lett. **106**, 080801 (2011).
14. T. Aoyama, M. Hayakawa, T. Kinoshita, and M. Nio, Phys. Rev. Lett. **109**, 111807 (2012).